ISBN: 978-3-95450-234-9 ISSN: 2673-5504 doi:10.18429/JACoW-SRF2023-MOPMB044

TOPOGRAPHIC EVOLUTION OF NITROGEN DOPED Nb SUBJECTED TO ELECTROPOLISHING*

E. M. Lechner[1,†], J. W. Angle[2], C. Baxley[1], M. J. Kelley[1,2], C. E. Reece[1]
[1]Thomas Jefferson National Accelerator Facility, Newport News, VA, USA
[2]Virginia Polytechnic Institute and State University, Blacksburg, VA, USA

Abstract

Surface quality is paramount in facilitating high performance SRF cavity operation. Here, we investigate the topographic evolution of samples subjected to N-doping and 600 °C vacuum anneal. We show that in N-doped Nb, niobium nitrides may grow continuously along grain boundaries. Upon electropolishing high slope angle grooves are revealed which sets up a condition that may facilitate a suppression of the superheating field.

INTRODUCTION

The N doping process [1] of thermally diffusing N at 800 °C in a low pressure N_2 environment has resulted in substantial decreases of the surface resistance at moderate accelerating gradients. Based on the reproducibility of the intended performance N doping was chosen for production cavities in the LCLS-II and LCLS-II HE upgrades. The LCLS-II HE research and development program investigated the performance of three N doping protocols [2]. It was shown that the process of N doping Nb cavities at 800 °C for two minutes in an N_2 atmosphere with no post-dope anneal (referred to as "2N0") was superior to cavities doped for 2 minutes and annealed for 6 minutes or doped for 3 minutes and annealed for 60 minutes. After N doping, a 7 µm electropolish is performed to recover performance. The N doping process is known to leave behind topographic defects due to the removal of nitrides during the electropolishing process [3]. Topographic defects are one vector that may reduce superheating fields either by magnetic field enhancement [4-6] or by nanoscale defects [7, 8]. Another source of degradation may be from impurities [9]. To investigate the possible topographic contribution we examine the topographic evolution of 2N0 N-doped and vacuum annealed Nb samples subjected to electropolishing using an atomic force microscope (AFM).

RESULTS

Here, we examine nitrogen doped and vacuum annealed (600 °C/10 hr) samples using atomic force microscopy after sequential electropolishing. Electropolishing (EP) was performed using a 1 to 10 by volume mixture of HF(49%) to H_2SO_4(98%). Samples of 6 × 10 × ~3 mm^3 were wrapped in PTFE tape, mounted in a sample holder and immersed in the EP electrolyte allowing only the polished face to be exposed to the electrolyte. Samples were electropolished at 13 °C and 9 V. Tapping-mode AFM topographies were made using a Digital Instruments Nanoscope IV atomic force microscope. The AFM probe tip used was a Si tip with a tip radius less than 10 nm.

The N doping process precipitates nitrides within grains and can precipitate nitrides along grain boundaries. During the electropolishing process nitrides are preferentially removed as shown in Fig. 1. Smaller holes are formed within grains while relatively deep grooves may be produced along grain boundaries. Electropolishing leaves behind long grooves along grain boundaries and reveals high slope angle areas. To study the evolution of topographic features we examined two 2N0 N doped samples and two electropolished samples for comparison. Representative intragrain tapping-mode atomic force microscope topographies are shown in Fig. 2 which shows the evolution of surface upon electropolishing. Some holes of approximately 1 µm in width are introduced into the 600 °C heat treated samples which are suspected to be due to growth of an unidentified Nb compound. With increasing electropolishing depth the holes tend to become more rounded and shallower. The evolution of average surface roughness S_a is shown in Fig. 3 for the 2N0 samples compared with 600 °C, 10 hour vacuum annealed samples.

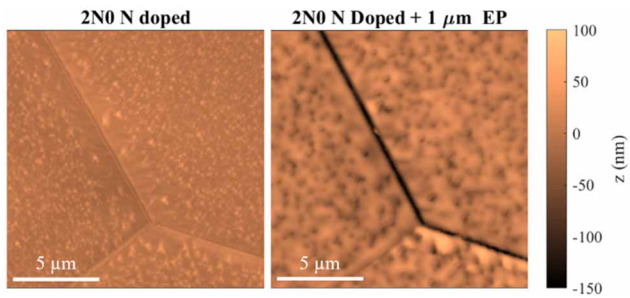

Figure 1: Before (left) and after (right) electropolishing at a triple-junction.

Along some grain boundaries, grooves are present which also become more rounded and shallower with electropolishing depth. The evolution of topography at triple junctions is shown in Fig. 4. A common defect observed at the grain boundary is a deeper removal of material around the triple-junction likely due to enhanced diffusion between grains. The geometry of the groove topographic defect is reminiscent of the triangular groove defect studied by Kubo [8]. Kubo's model predicts a superheating field suppression from nanoscale features of the surface and the superconductor's coherence length. The suppression of the superheating field is dependent on the triangular groove

* Work supported by U.S. DOE contract DE-AC05-06OR23177
† lechner@jlab.org

ISBN: 978-3-95450-234-9 ISSN: 2673-5504 doi:10.18429/JACoW-SRF2023-MOPMB044

slope angle, θ, depth of the groove, δ and the superconductor's coherence length, ξ. The superheating field suppression factor η, defined by $\tilde{B}_s = \eta B_s$ is calculated by

$$\eta = \frac{1}{\alpha}\left(\frac{\left(\Gamma\left(\frac{\alpha}{2}\right)\Gamma\left(\frac{3-\alpha}{2}\right)\alpha\sin\left(\frac{\pi(\alpha-1)}{2}\right)\right)}{\sqrt{\pi}}\frac{\xi}{\delta}\right)^{\frac{\alpha-1}{\alpha}} \quad (1)$$

where α is defined by $\theta = \pi(\alpha-1)/2$. Towards calculating Eq. (1) from topography, a local slope angle which quantifies the angular deviation of the surface plane from the x-y plane can be calculated using the tapping-mode AFM topographies, $z = h(x,y)$ by

$$\cos\theta = \hat{\boldsymbol{z}}\cdot\hat{\boldsymbol{n}} = \hat{\boldsymbol{z}}\cdot\frac{(-h_x,-h_y,1)}{(1+h_x^2+h_y^2)^{\frac{1}{2}}} \quad (2)$$

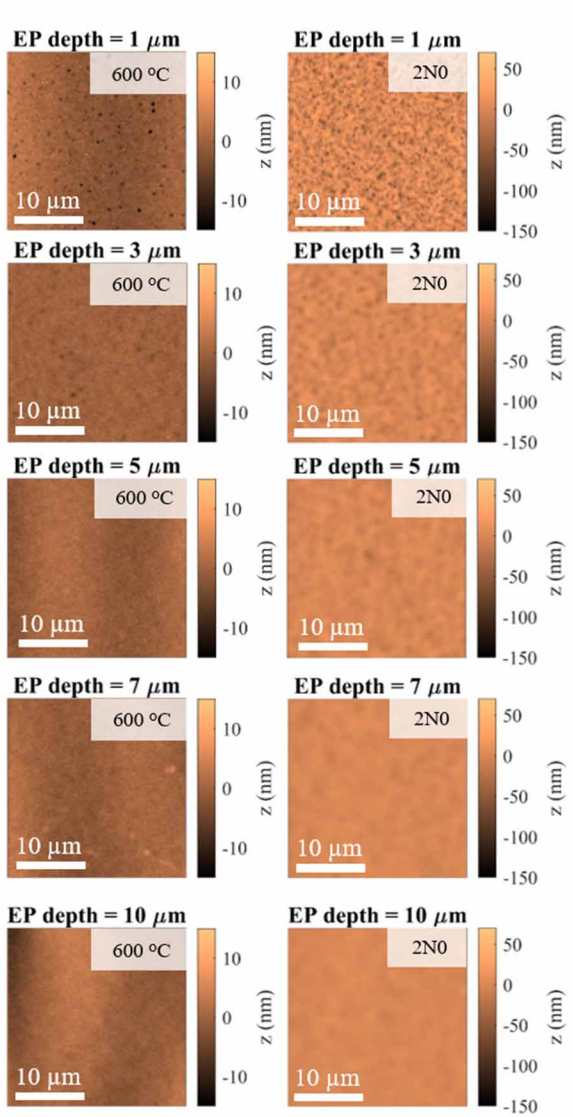

Figure 2: Representative intragrain tapping-mode AFM topography for 600 °C heat treated and 2N0.

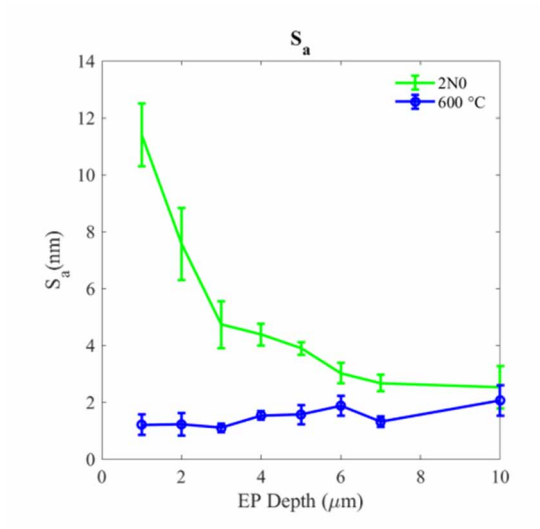

Figure 3: Evolution of average intragrain surface roughness, S_a, with electropolishing depth.

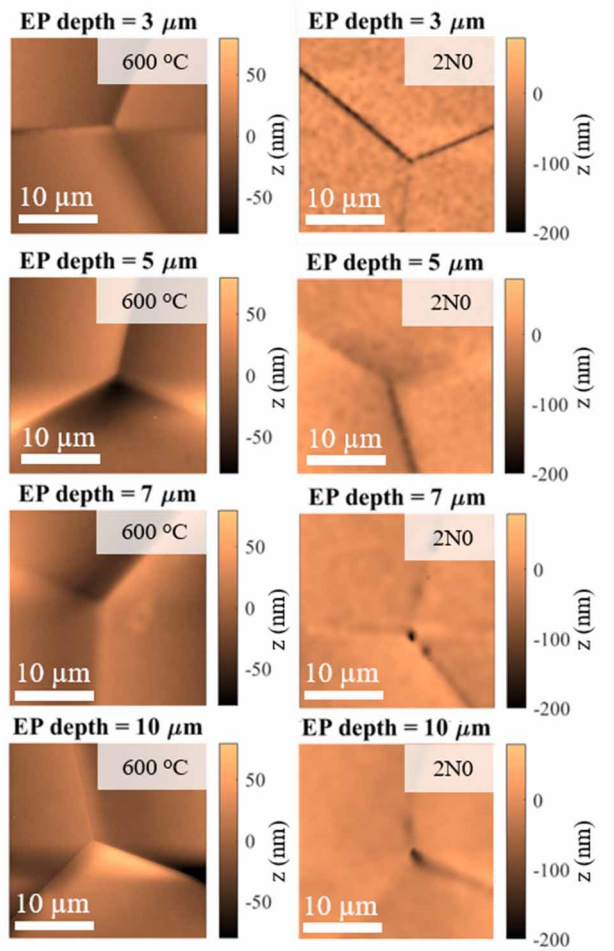

Figure 4: Representative triple-junction tapping-mode AFM topography for 600 °C heat treated and 2N0.

where $\hat{\boldsymbol{n}}$ is the unit normal vector to the measured surface, h_i is the partial derivative of h with respect to coordinate i [10]. Partial derivatives of $h(x,y)$ were calculated using an extension of the Savitzky-Golay filtering method for

ISBN: 978-3-95450-234-9 ISSN: 2673-5504 doi:10.18429/JACoW-SRF2023-MOPMB044

surfaces [11, 12]. To estimate the depth of the holes and grooves we define $\delta(\boldsymbol{r})$ as the difference between the AFM topography and a fitted plane that conforms to surface without conforming to the holes and defects. ξ is estimated at 20 nm for the N doped samples and 40 nm for the 600 °C heat treated samples. While entrance of vortices should occur at the valley minima, the grain boundary grooves present slope angles that are not constant throughout and often the grooves observed have depths comparable to the length scale of the penetration depth which deviates from Kubo's model assumptions. With these limitations in mind, we utilize Eq. (1) using $\alpha(\boldsymbol{r})$, $\xi\ \delta(\boldsymbol{r})$ to calculate $\eta(\boldsymbol{r})$. We note that $\eta(\boldsymbol{r})$ does not represent a local superheating field suppression factor except in some cases near minima. A representative topography, slope angle map, $\eta(\boldsymbol{r})$ map for is shown in Fig. 5.

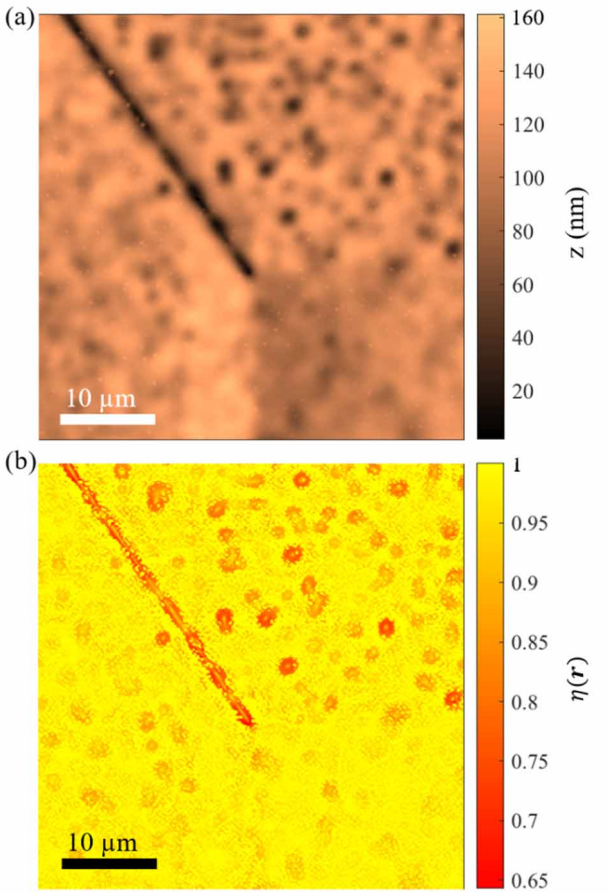

Figure 5: (a) Tapping-mode AFM topography and (b) calculation of $\eta(\boldsymbol{r})$ for a 2N0 triple junction after 3 μm electropolish.

Plots of the relative frequency of $\eta(\boldsymbol{r})$ with electropolishing depth, shown in Fig. 6, reveal a wider distribution of $\eta(\boldsymbol{r})$ values in the N doped samples which is ameliorated with more electropolishing.

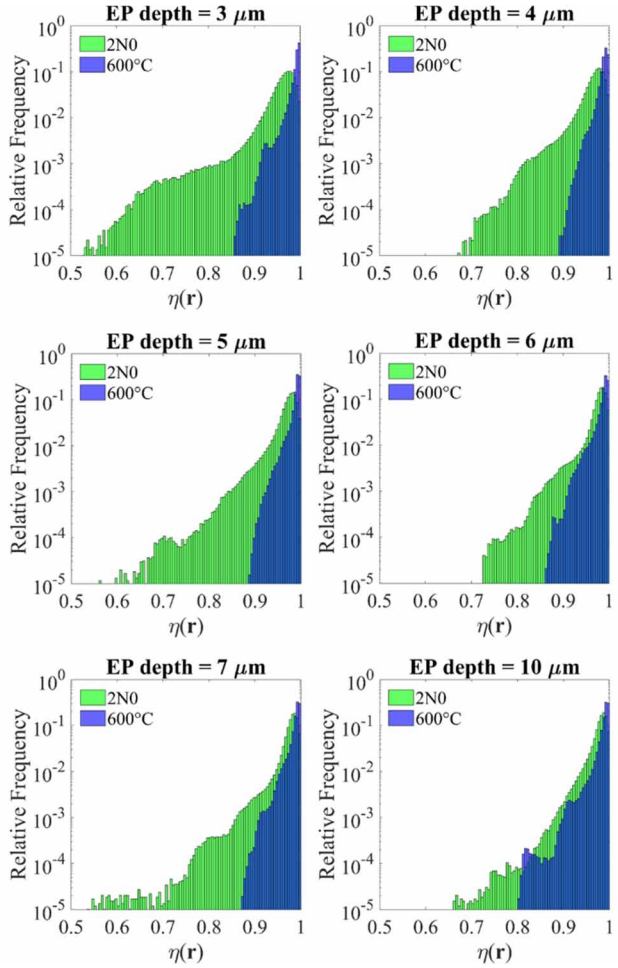

Figure 6: Relative frequency of $\eta(\boldsymbol{r})$ for 2N0 and 600 °C heat treated triple-junction topographies with electropolishing depth.

CONCLUSION

We have shown that the preferential removal of nitrides during electropolishing introduces topographic defects that may facilitate vortex penetration via superheating field suppression. Our quantitative estimates for the decrease in superheating field are complicated by the limitations of available theories, but qualitative comparisons between heat treatment processes may be possible. It's clear in the limit of deep grooves, that as a material moves deeper into the type-II regime it becomes substantially more sensitive to topographic defects for flux entry [7]. The analysis outlined here will be useful for materials with larger penetration depths in comparison with their topographic defects or for improving polishing processes of interest for SRF applications [13-15].

Ideally after N doping a long electropolish to remove the topographic defects would be employed, however the N diffusion lengths are not long enough to accommodate this. As an example, for the 2N0 recipe, the N diffusion profile is relatively short which means going from a 7 μm to 10 μm EP could be beneficial for max accelerating gradient but come at a cost of reducing interstitials from approxi-

ISBN: 978-3-95450-234-9 ISSN: 2673-5504 doi:10.18429/JACoW-SRF2023-MOPMB044

mately 1000 ppm to 800 ppm [16] which should reduce efficiency. Longer impurity diffusion profiles that change negligibly in concentration during electropolishing would be ideal to negate the effects of topographic defects introduced during doping.

ACKNOWLEDGEMENTS

This material is based on work supported by the U.S. Department of Science, Office of Science, Office of Nuclear Physics Early Career Award to A. Palczewski. J. Angle's support was from the Office of High Energy Physics, under grant DE-SC-0014475 to Virginia Tech.

REFERENCES

[1] A. Grassellino *et al.*, "Nitrogen and argon doping of niobium for superconducting radio frequency cavities: a pathway to highly efficient accelerating structures," *Supercond. Sci. Technol.,* vol. 26, no. 10, p. 102001, 2013. doi:10.1088/0953-2048/26/10/102001

[2] D. Gonnella *et al.*, "The LCLS-II HE High Q and Gradient R&D *Program*," in *Proc. SRF'19*, Dresden, Germany, Jun.-Jul. 2019, pp. 154-158. doi:10.18429/JACoW-SRF2019-MOP045

[3] J. Spradlin, A. Palczewski, H. Tian, and C. Reece, "Analysis of Surface Nitrides Created During "Doping" Heat Treatments of Niobium," in *Proc. SRF'19*, Dresden, Germany, Jun.-Jul. 2019, pp. 106-111. doi:10.18429/JACoW-SRF2019-MOP030

[4] J. Knobloch, R. Geng, M. Liepe, and H. Padamsee, "High-field Q slope in superconducting cavities due to magnetic field enhancement at grain boundaries," in *Proc. SRF'99*, Santa Fe, NM, USA, Nov. 1999, paper TUA004, pp. 77-91.

[5] T. Kubo, "Magnetic field enhancement at a pit on the surface of a superconducting accelerating cavity," *Prog. Theor. Exp. Phys,* vol. 2015, no. 7, 2015. doi:10.1093/ptep/ptv088

[6] C. Xu, C. E. Reece, and M. J. Kelley, "Simulation of nonlinear superconducting rf losses derived from characteristic topography of etched and electropolished niobium surfaces," *Phys. Rev. Accel. Beams,* vol. 19, no. 3, p. 033501, 2016. doi:10.1103/PhysRevAccelBeams.19.033501

[7] A. Y. Aladyshkin, A. Mel'nikov, I. Shereshevsky, and I. Tokman, "What is the best gate for vortex entry into type-II superconductor?," *Phys. C: Supercond. Appl.,* vol. 361, no. 1, pp. 67-72, 2001. doi:10.1016/S0921-4534(01)00288-X

[8] T. Kubo, "Field limit and nano-scale surface topography of superconducting radio-frequency cavity made of extreme type II superconductor," *Prog. Theor. Exp. Phys,* vol. 2015, no. 6, 2015. doi:10.1093/ptep/ptv082

[9] T. Kubo, "Effects of Nonmagnetic Impurities and Subgap States on the Kinetic Inductance, Complex Conductivity, Quality Factor, and Depairing Current Density," *Phys. Rev. Appl.,* vol. 17, no. 1, p. 014018, 2022. doi:10.1103/PhysRevApplied.17.014018

[10] M. P. Do Carmo, *Differential geometry of curves and surfaces*, revised and updated second edition. Courier Dover Publications, 2016.

[11] J. E. Kuo, H. Wang, and S. Pickup, "Multidimensional least-squares smoothing using orthogonal polynomials," *Anal. Chem*., vol. 63, no. 6, pp. 630-635, 1991. doi:10.1021/ac00006a015

[12] A. Savitzky and M. J. Golay, "Smoothing and differentiation of data by simplified least squares procedures," *Anal. Chem*., vol. 36, no. 8, pp. 1627-1639, 1964 doi:10.1021/ac60214a047

[13] U. Pudasaini, G. V. Eremeev, J. W. Angle, J. Tuggle, C. E. Reece, and M. J. Kelley, "Growth of Nb_3Sn coating in tin vapor-diffusion process," *J. Vac. Sci. Technol. A*, vol. 37, no. 5, p. 051509, 2019. doi:10.1116/1.5113597

[14] C. Pira *et al*., "Impact of the Cu substrate surface preparation on the morphological, superconductive and RF properties of the Nb superconductive coatings," in *Proc. SRF'19*, Dresden, Germany, Jun.-Jul. 2019, pp. 935-940. doi:10.18429/JACoW-SRF2019-THP041

[15] A.-M. Valente-Feliciano, "Superconducting RF materials other than bulk niobium: a review," *Supercond. Sci. Technol*., vol. 29, no. 11, p. 113002, 2016. doi:10.1088/0953-2048/29/11/113002

[16] C. Reece, E. Lechner, M. Kelley, and J. Angle, "SIMS Characterization of Nitrogen Doping of LCLS-II-HE Production Cavities," presented at SRF'23, Grand Rapids, MI, USA, Jun. 2023, paper MOPMB006, this conference.